Control of Non-linear Marine Cooling System

Michael Hansen, Jakob Stoustrup, Jan Dimon Bendtsen

***Abstract*— We consider the problem of designing control laws for a marine cooling system used for cooling the main engine and auxiliary components aboard several classes of container vessels. We focus on achieving simple set point control for the system and do not consider compensation of the non-linearities, closed circuit flow dynamics or transport delays that are present in the system. Control laws are therefore designed using classical control theory and the performance of the design is illustrated through a simulation example where it is compared to a reference control design.**

I. INTRODUCTION

In recent years the attention to energy efficiency in the shipping industry has increased as a consequence of fluctuating oil prices [1] and a growing focus on CO_2, NO_x and SO_x emissions from maritime transportation [2]. This has led to several initiatives within the shipping industry to bring down the energy consumption in ocean-going vessels, ranging from waste heat recovery systems to energy optimization of subsystems [3].

In this paper we consider design of control laws for a cooling system found aboard several classes of ocean-going container vessels. The system in question is used for cooling the main engine and auxiliary components and currently makes use of a very simple control method. In the current control, the pumps in the cooling system are operated in three steps based on the temperature of the sea water and the load on the main engine [4]. The result is that the pumps in this type of cooling system are used excessively, and that operating conditions are unlikely to be optimal in particular for the main engine auxiliary components. This leaves a significant potential for energy savings by improving the existing controls, not only by lowering the power consumption of the pumps, but also by ensuring optimal operating conditions for the main engine auxiliary components and thereby improving their energy efficiency. The focus in this paper is on the latter, which means that the control design aims at achieving the desired set point temperatures for main engine auxiliary components, rather than achieving optimal energy efficiency for the pumps.

A model for the cooling system was derived in [5] and is adopted here for the control design and for simulating the compensated system. The control laws derived in this paper serves the purpose of improving the performance of the cooling system compared to the current control method.

The remainder of the paper is structured as follows: In Section II we give a short description of the system and present the model. In Section III we present the control strategy and derive control laws for the system. Section IV presents simulation results for the control design and conclusions are given in Section V.

M. Hansen is with A.P. Moeller - Maersk A/S, MMT - Innovation, Esplanaden 50, DK-1098, Copenhagen, Denmark and is also affiliated with the Department of Electronic Systems, Section for Automation and Control, Aalborg University, Fredrik Bajers Vej 7, DK-9320, Aalborg, Denmark (e-mail: michael.hansen1@maersk.com).

Jakob Stoustrup and Jan Dimon Bendtsen are with the Department of Electronic Systems, Section for Automation and Control, Aalborg University, Fredrik Bajers Vej 7, DK-9320, Aalborg, Denmark (e-mail: {jakob, dimon}@es.aau.dk)

II. MODEL

The cooling system consists of three circuits; a sea water (SW) circuit, a low temperature (LT) circuit and a high temperature (HT) circuit. This is illustrated in Fig. 1 where q_{LT} and q_{SW} are volumetric flows in the LT and SW circuits, while q_{HT} is the volumetric flow to the HT circuit.

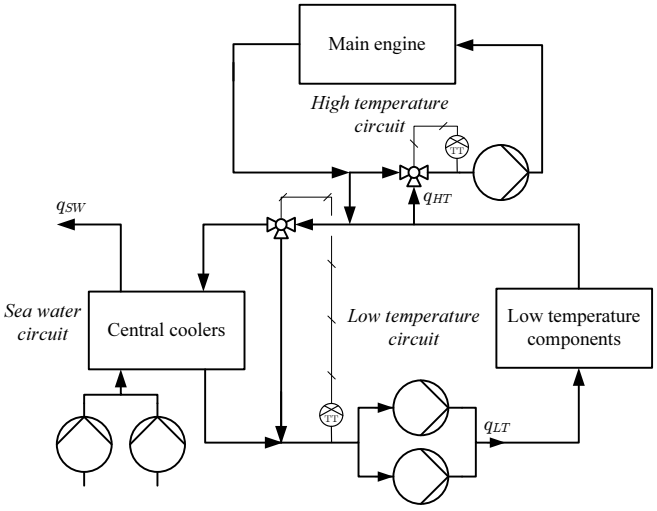

Fig. 1. Simplified system layout.

The SW circuit pumps sea water through the cold side of the central coolers for lowering the temperature of the coolant in the LT and HT circuits. The HT circuit only contains the main engine of the ship, while the LT circuit contains all the main engine auxiliary components in a parallel configuration. In the current control scheme, the SW circuit pumps are operated in three steps depending on the temperature of the sea water and the operating mode of the vessel. This setup is designed such that the SW circuit provides sufficient cooling, even when the sea water temperature is high, which means that under most operating conditions the SW circuit generates excess cooling. Similar to the SW pumps, the LT pumps are also controlled in

three steps and the pump setting is determined by the sea water temperature, the operating mode of the vessel, and the main engine load percentage. There is a requirement for the temperature of the coolant to be at least 36°C at the inlet of some consumers, which is ensured by a temperature controller that adjusts the amount of coolant that is flowing through the shunt, past the central coolers.

We employ a model for the cooling system constructed in [5], and essential parts are repeated here for convenience. The model consists of two parts; one describing the hydraulics and one describing the thermodynamics.

A. Hydraulics

The hydraulic model describes the flow in the SW circuit and LT circuit respectively. The equation governing the flow in the SW circuit is given by:

$$J_{sw}\dot{q}_{sw} = -K_{sw}|q_{sw}|q_{sw} - \Delta h_{io} + \Delta h_{p,sw} \ , \qquad (1)$$

where J_{sw} and K_{sw} are pipe section parameters, q_{sw} is the volumetric flow, Δh_{io} is the pressure drop due to difference in height from the sea water intake and outlet, and $\Delta h_{p,sw}$ is the delivered pump head.

The hydraulic model for the LT circuit was originally adopted from [6] and we use the same notation and definitions here. This means that we model valves as:

$$h_i - h_j = K_v|q_v|q_v \ , \qquad (2)$$

where $(h_i - h_j)$ is the pressure drop across the valve, K_v is a variable describing the hydraulic resistance of the valve, and q_v is the volumetric flow through the valve. As a remark we introduce the index $\{cv\}$ for controllable valves to distinguish them from non-controllable valves, which we denote by index $\{v\}$. Pipes are modeled as:

$$J\frac{dq_p}{dt} = (h_i - h_j) - K_p|q_p|q_p \ , \qquad (3)$$

where J and K_p are constant parameters for the pipe section, $(h_i - h_j)$ is the pressure drop along the pipe and q_p is the flow through the pipe. Finally, pumps are modeled by:

$$h_i - h_j = -\Delta h_p \ , \qquad (4)$$

where $(h_i - h_j)$ is the pressure across the pump and Δh_p is the delivered pump head. In the design presented in this paper we assume that the LT circuit contains only two consumers, resulting in a hydraulic structure as illustrated in Fig. 2.

The model for the circuit illustrated in Fig. 2 is derived using network theory and by applying the analogy between electrical and hydraulic circuits where voltage and currents corresponds to pressure and flows. Since we will only sketch the modeling approach here, the interested reader can refer to [6] and [7] for a more general and detailed description. By inspection, it is possible to identify two independent flows in Fig. 2, namely q_1 and q_2. Using the electrical circuit analogy we can exploit Kirchhoffs voltage law for the two

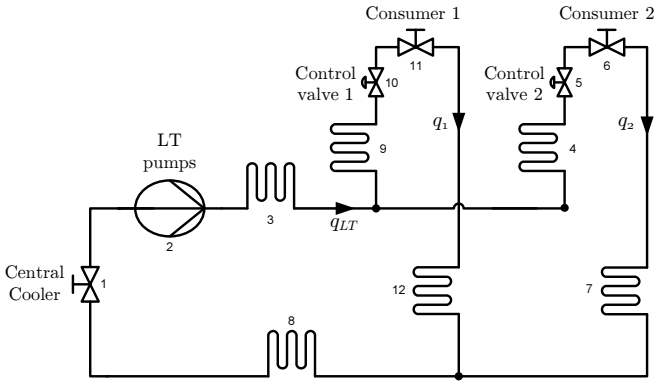

Fig. 2. Assumed hydraulic structure for the LT circuit in this design example.

fundamental loops that includes q_1 and q_2, by which we achieve:

$$\begin{aligned} 0 = &-\Delta h_1 + \Delta h_2 - \Delta h_3 - \Delta h_4 - \Delta h_5 - \Delta h_6 \\ &- \Delta h_7 - \Delta h_8 \ , \end{aligned} \qquad (5)$$

$$\begin{aligned} 0 = &-\Delta h_1 + \Delta h_2 - \Delta h_3 - \Delta h_9 - \Delta h_{10} - \Delta h_{11} \\ &- \Delta h_{12} - \Delta h_8 \ , \end{aligned} \qquad (6)$$

where Δh_i is the pressure across component i in Fig. 2. Each pressure term in (5) and (6) is replaced by its corresponding model from (2)-(4). Realizing that the individual component flows can be written as a linear combination of the independent flows q_1 and q_2 and assuming that flows are always positive, i.e., $q_1 \geq 0$ and $q_2 \geq 0$, we get that:

$$\begin{aligned} 0 = &-(K_{v1} + K_{p3} + K_{p8})(q_1^2 + q_2^2) - (J_3 + J_8)\frac{d(q_1 + q_2)}{dt} \\ &- (J_4 + J_7)\frac{dq_2}{dt} - (K_{p4} + K_{cv5} + K_{v6} + K_{p7})q_2^2 \\ &+ \Delta h_p \ , \end{aligned} \qquad (7)$$

$$\begin{aligned} 0 = &-(K_{v1} + K_{p3} + K_{p8})(q_1^2 + q_2^2) - (J_3 + J_8)\frac{d(q_1 + q_2)}{dt} \\ &- (J_9 + J_{12})\frac{dq_1}{dt} - (K_{p9} + K_{cv10} + K_{v11} + K_{p12})q_1^2 \\ &+ \Delta h_p \ . \end{aligned} \qquad (8)$$

Through some tedious but straightforward calculations it is possible obtain the following expressions for the dynamics of the flows q_1 and q_2:

$$\dot{q}_1 = -K_{11}q_1^2 - K_{12}q_1^2\varphi_{cv1} + K_{13}q_2^2\varphi_{cv2} + K_{14}\Delta h_p \ , \qquad (9)$$

$$\dot{q}_2 = -K_{21}q_2^2 - K_{22}q_2^2\varphi_{cv2} + K_{23}q_1^2\varphi_{cv1} + K_{24}\Delta h_p \ , \qquad (10)$$

where $K_{11}, K_{12}, K_{13}, K_{14}, K_{21}, K_{22}, K_{23}$ and K_{24} are all positive circuit specific parameters, while $\varphi_{cv1} = K_{cv10}$ and $\varphi_{cv2} = K_{cv5}$ denotes the hydraulic resistances of control valve 1 and 2, respectively.

B. Thermodynamics

The thermodynamic model derived in [5] includes flow dependent delays and also models how the coolant is recirculated in the system. Though a possible approach would

be to linearize the delays and include them in the control design presented here, it is chosen not to as the purpose here is to design simple baseline control laws, while later work will consider compensation of delays and closed circuit flow behavior. The thermodynamic model applied for control design in this paper therefore consists of two equations; one governing the dynamics of the central cooler, and one governing the dynamics of the consumers in the LT circuit. For consumer $i = 1, \ldots, n$ in the LT circuit we have that:

$$\frac{d\,T_i(t)}{dt} = \frac{1}{\rho c_p V_i}\left(q_i(t)\rho c_p(T_{in}(t) - T_i(t)) + \dot{Q}_i(t)\right) \ , \tag{11}$$

where q_i is the volumetric flow rate through the consumer, V_i is the internal volume of the consumer, T_i is the outlet temperature of the consumer, T_{in} is the outlet temperature of the central cooler (into the LT circuit), $\dot{Q}_i$ is the heat transfer from the consumer, ρ is the density of the coolant and c_p is the specific heat of the coolant.

For the central cooler we have that:

$$\begin{aligned}\frac{d\,T_{in}(t)}{dt} =& \frac{1}{\rho c_p V_{CC}}\left[q_{LT}(t)\rho c_p(T_{CC,in}(t) - T_{in}(t))\right. \\ &\left. + \ q_{SW}(t)\rho_{sw}c_{p,sw}(T_{SW,in}(t) - T_{SW,out}(t)\right] \ ,\end{aligned} \tag{12}$$

where $T_{CC,in}$ is the inlet temperature of the central cooler on the LT side, $T_{SW,in}$ is the inlet temperature of the central cooler on the SW side and $T_{SW,out}$ is the outlet temperature of the central cooler on the SW side. Also, q_{LT} is the volumetric flow rate through the LT side of the central cooler, q_{SW} is the volumetric flow rate through the SW side of the central cooler, V_{CC} is the internal volume of the central cooler, ρ_{sw} is the density of the sea water and $c_{p,sw}$ is the specific heat of the sea water.

Equations (1) and (9)-(10) constitutes the hydraulic model for the SW and LT circuit respectively, while equations (11) and (12) make up the thermodynamic model.

III. CONTROL DESIGN

The control design is divided into two parts; control laws for the SW circuit and control laws for the LT circuit. Furthermore, since both the SW and LT circuit can be considered as a hydraulic part cascaded with a thermodynamic part we use a cascaded control design for both circuits as illustrated in Fig. 3.

A. Design of Flow Controllers

The purpose of the flow controllers is to assure that the flows in the system tracks the references given by the temperature controllers. We start by designing the controller for the flow in the SW circuit, q_{sw}, using the model given by (1). We again assume that the flow is only going in one direction, i.e. $q_{sw} \geq 0$. We can now rewrite (1) and obtain:

$$\dot{q}_{sw} = \frac{1}{J_{sw}}\left(-K_{sw}q_{sw}^2 - \Delta h_{io} + \Delta h_{p,sw}\right) \ . \tag{13}$$

A linearized small perturbation model is obtained using a first order Taylor expansion:

$$\frac{d\,\hat{q}_{sw}}{dt} = \frac{1}{J_{sw}}\left(-2K_{sw}\bar{q}_{sw}\hat{q}_{sw} + \Delta\hat{h}_{p,sw}\right) \ , \tag{14}$$

where we use $\bar{q}_{sw}$ to denote the steady state value of q_{sw} and $\hat{q}_{sw}$ to denote a small perturbation from the steady state value of q_{sw}. The same notation applies for $\Delta h_{p,sw}$. The transfer function from delivered pump head, $\Delta h_{p,sw}$ to the SW flow rate, q_{sw} is according to Equation (14) given by:

$$G_{sw}(s) = \frac{\hat{q}_{sw}(s)}{\Delta\hat{h}_{p,sw}(s)} = \frac{\frac{1}{2K_{sw}\bar{q}_{sw}}}{s\frac{J_{sw}}{2K_{sw}\bar{q}_{sw}} + 1} \ . \tag{15}$$

In this design example we use $K_{sw} = 10$, $\bar{q}_{sw} = 0.183$ and $J_{sw} = 1$. We pursue a standard PI controller design, given in the form of:

$$D(s) = K_p\left(1 + \frac{1}{sT_i}\right) \ . \tag{16}$$

As design parameters for all flow controllers we use phase margin and crossover frequency and make the choice of $PM = 70^\circ$ at $\omega_0 = 0.4$ rad/s. From the requirements for phase margin and crossover frequency we can determine K_p and T_i from [8]:

$$|D(s)G(s)|_{s=j\omega_0} = 1 \ , \tag{17}$$

$$\tan^{-1}\left(\frac{\mathrm{Im}(D(s)G(s))}{\mathrm{Re}(D(s)G(s))}\right)\Bigg|_{s=j\omega_0} = PM - 180^\circ \ . \tag{18}$$

By inserting (15) and (16) into (17) and (18) we can solve for K_p and T_i, which for the SW flow controller yields:

$$D_{sw}(s) = -0.88\left(1 - \frac{1}{0.61s}\right) \ . \tag{19}$$

For the LT circuit flow we have the linearized small perturbation versions of (9) and (10) given by:

$$\begin{aligned}\frac{d\,\hat{q}_1}{dt} =& \ \hat{q}_1(-2K_{11}\bar{q}_1 - 2K_{12}\bar{q}_1\bar{\varphi}_{cv1}) + \hat{q}_2(2K_{13}\bar{q}_2\bar{\varphi}_{cv2}) \\ &- \hat{\varphi}_{cv1}(K_{12}\bar{q}_1^2) + \hat{\varphi}_{cv2}(K_{13}\bar{q}_2^2) + K_{14}\Delta\hat{h}_{p,LT} \ ,\end{aligned} \tag{20}$$

$$\begin{aligned}\frac{d\,\hat{q}_2}{dt} =& \ \hat{q}_2(-2K_{21}\bar{q}_2 - 2K_{22}\bar{q}_2\bar{\varphi}_{cv2}) + \hat{q}_1(2K_{23}\bar{q}_1\bar{\varphi}_{cv1}) \\ &- \hat{\varphi}_{cv2}(K_{22}\bar{q}_2^2) + \hat{\varphi}_{cv1}(K_{23}\bar{q}_1^2) + K_{24}\Delta\hat{h}_{p,LT} \ .\end{aligned} \tag{21}$$

Assuming that we use φ_{cv1} to control q_1 and φ_{cv2} to control q_2 we leave out cross-coupling terms in (20)-(21) and by the Laplace transform we achieve the following transfer functions:

$$G_{q1}(s) = \frac{\hat{q}_1(s)}{\hat{\varphi}_{cv1}(s)} = \frac{-K_{12}\bar{q}_1^2}{s + (2K_{11}\bar{q}_1 + 2K_{12}\bar{q}_1\bar{\varphi}_{cv1})} \ , \tag{22}$$

$$G_{q2}(s) = \frac{\hat{q}_2(s)}{\hat{\varphi}_{cv2}(s)} = \frac{-K_{22}\bar{q}_2^2}{s + (2K_{21}\bar{q}_2 + 2K_{22}\bar{q}_2\bar{\varphi}_{cv2})} \ . \tag{23}$$

For this design example we use the hydraulic parameters presented in Table I.

Just as for the SW flow controller design we pursue a PI compensator as given by (16) using the same design parameters. As before we determine K_p and T_i for the

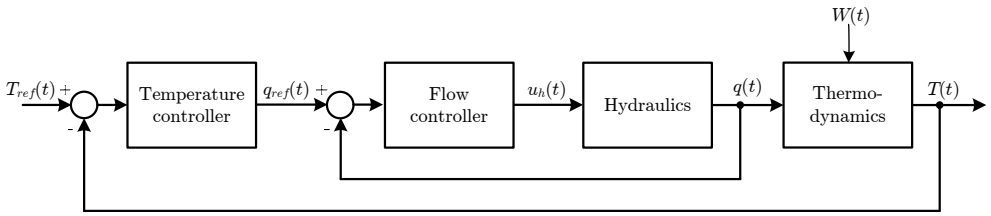

Fig. 3. Block diagram for the cascaded control setup. u_h denotes the hydraulic inputs, i.e. φ_{cv1}, φ_{cv2}, $h_{p,sw}$ and $h_{p,LT}$. $W(t)$ denotes the disturbances to the thermodynamics of the system, such as $\dot{Q}_1$, $\dot{Q}_2$ and $T_{sw,in}$.

TABLE I

HYDRAULIC PARAMETERS FOR LT CIRCUIT.

K_{11}	K_{12}	K_{13}	K_{14}	$\bar{q}_1$	$\bar{\varphi}_{cv1}$
15	$\frac{1}{3}$	$\frac{1}{6}$	$\frac{1}{6}$	0.050	3820
K_{21}	K_{22}	K_{23}	K_{24}	$\bar{q}_2$	$\bar{\varphi}_{cv2}$
15	$\frac{1}{3}$	$\frac{1}{6}$	$\frac{1}{6}$	0.042	5013

LT flow controllers from (17) and (18) using the transfer functions given by (22) and (23). With the parameters in Table I this yields:

$$D_{q1}(s) = 2.77 \times 10^3 \left(1 - \frac{1}{0.77s}\right) , \tag{24}$$

$$D_{q2}(s) = 3.53 \times 10^3 \left(1 - \frac{1}{0.76s}\right) . \tag{25}$$

This completes the design for the flow controllers.

B. Design of Temperature Controllers

The temperature controllers serve the purpose of keeping the LT circuit inlet temperature, $T_{in}(t)$, and the outlet temperature of the consumers, $T_1(t), \ldots, T_n(t)$, at a specified reference. Since the system operates in steady state mode for extended periods at a time, it is important to achieve zero steady state error for the temperatures in the system. Therefore we use a regular PI controller design for each control loop to remove steady state errors. We again use phase margin and crossover frequency as design parameters for the PI compensator and we choose $PM = 70^\circ$ and $\omega_0 = 0.002$ rad/s in the design of the consumer outlet temperature controllers. For the LT inlet temperature controller we choose $PM = 70^\circ$ and $\omega_0 = 0.01$ rad/s such that the dynamics of the LT inlet temperature is faster than the consumer outlet temperature but still significantly slower than the dynamics of the hydraulics.

Starting with the control design for the consumer outlet temperature, we make a first order Taylor expansion of Equation (11) to achieve the linearized small perturbation model given by:

$$\frac{d\,\hat{T}_i}{dt} = \frac{1}{V_i}\left(\hat{q}_i(\bar{T}_{in} - \bar{T}_i) + \bar{q}_i(\hat{T}_{in} - \hat{T}_i) + \frac{\hat{Q}_i}{\rho c_p}\right) . \tag{26}$$

The transfer functions from the flows to the consumer outlet temperatures are given by:

$$G_{T1}(s) = \frac{\hat{T}_1(s)}{\hat{q}_1(s)} = \frac{\frac{1}{\bar{q}_1}(\bar{T}_{in} - \bar{T}_1)}{s\frac{V_1}{\bar{q}_1} + 1} , \tag{27}$$

$$G_{T2}(s) = \frac{\hat{T}_2(s)}{\hat{q}_2(s)} = \frac{\frac{1}{\bar{q}_2}(\bar{T}_{in} - \bar{T}_2)}{s\frac{V_2}{\bar{q}_2} + 1} . \tag{28}$$

We use a regular PI design as given by Equation (16) and apply the same design procedure as for the flow controllers. Thermodynamic parameters used for this design example are illustrated in Table II.

TABLE II

THERMODYNAMIC PARAMETERS FOR COOLING SYSTEM.

c_p	$\dot{Q}_1$	ρ	$\bar{T}_{sw,in}$	V_{cc}	V_1	$\bar{T}_1$	$\bar{q}_{LT}$
4181	6×10^6	1000	24	20	13.5	65	0.09
$c_{p,sw}$	$\dot{Q}_2$	ρ_{sw}	$\bar{T}_{sw,out}$	$\bar{T}_{in}$	V_2	$\bar{T}_2$	$\bar{T}_{cc,in}$
3993	6×10^6	1025	40	36	13.5	70	67.8

The temperature controllers for the consumer outlet temperature are then given by:

$$D_{T1}(s) = -2.91 \times 10^{-4}\left(1 + \frac{1}{75.78s}\right) , \tag{29}$$

$$D_{T2}(s) = -6.81 \times 10^{-4}\left(1 + \frac{1}{111.83s}\right) . \tag{30}$$

For the control of the LT inlet temperature we linearize the model given by (12), by which we obtain:

$$\begin{aligned}\frac{d\,\hat{T}_{in}}{dt} = \frac{1}{\rho c_p V_{cc}} \Big[&\hat{q}_{LT} c_p \rho (\bar{T}_{cc,in} - \bar{T}_{in}) + \hat{T}_{cc,in} c_p \rho \bar{q}_{LT} \\ &- \hat{T}_{in} c_p \rho \bar{q}_{LT} + \hat{q}_{sw} c_{p,sw} \rho_{sw} (\bar{T}_{sw,in} - \bar{T}_{sw,out}) \\ &+ \hat{T}_{sw,in} c_{p,sw} \rho_{sw} \bar{q}_{sw} - \hat{T}_{sw,out} c_{p,sw} \rho_{sw} \bar{q}_{sw} \Big] .\end{aligned} \tag{31}$$

The transfer function from the SW flow rate to the LT inlet temperature is given by:

$$G_{Tin}(s) = \frac{\hat{T}_{in}(s)}{\hat{q}_{sw}(s)} = \frac{\frac{c_{p,sw}\rho_{sw}(\bar{T}_{sw,in} - \bar{T}_{sw,out})}{\rho c_p \bar{q}_{LT}}}{\left(s\frac{V_{cc}}{\bar{q}_{LT}} + 1\right)} . \tag{32}$$

Using the parameters given by Table II and applying the the same design procedure as for the LT consumer outlet temperature, we achieve the following compensator design:

$$D_{Tin}(s) = -0.01\left(1 + \frac{1}{101.30s}\right) . \tag{33}$$

This completes the design for the temperature controllers.

IV. SIMULATION RESULTS

The controllers designed in Section III are assessed through a simulation study using the non-linear model derived in [5]. For comparison, we also simulate a control design that is similar to what is currently implemented on the cooling system. Both control designs are subject to the same conditions and disturbances, and the idea is to show how the design derived in this paper compares to a design that is close to the current implementation. The comparison control operates the LT pumps in a stepwise manner based on the main engine load percentage, $\text{ME}_{load}(t)$, and the sea water temperature, $T_{sw,in}(t)$. This is similar to the control implemented on the cooling system today, but instead of controlling the LT inlet temperature using the three-way valve as described in Section II, we use the corresponding control derived in this paper.

In the simulation scenario constructed here, the comparison control has two modes of operation for the LT pumps: one pump running or two pumps running in parallel. The mode of operation depends on the relation:

$$\begin{aligned} &\text{1 pump running if:} \quad \text{ME}_{load}(t) < -2T_{sw,in}(t) + 134 \\ &\text{2 pumps running if:} \quad \text{ME}_{load}(t) \geq -2T_{sw,in}(t) + 134 \end{aligned}$$

The relation between the main engine load percentage and the total power dissipated in both consumers is linearly approximated in the interval that is of interest in this context by:

$$\text{ME}_{load}\frac{2}{5} \times 10^6 - 16 \times 10^6 \ .$$

In the simulations, the two control designs undergoes the same steps in the main engine load percentage; first from 70% to 90% at time $t = 2000$ s and then from 70% to 60% at time $t = 12000$ s. It is assumed that the heat is dissipated equally in the two consumers, which means that the load percentage of 70% corresponds to the operating point chosen for the consumer outlet temperature controller design. Additional simulation parameters are illustrated in Table III.

TABLE III

PARAMETERS FOR SIMULATION EXAMPLES. PARAMETERS MARKED WITH * DENOTES SYSTEM SPECIFIC DELAY PARAMETERS FOR THE NON-LINEAR MODEL, SEE [5] FOR DETAILS.

$T_{1,ref}$	$T_{2,ref}$	$T_{in,ref}$	$T_{sw,in}$	$T_{sw,out}$
65	70	36	24	40
$a_{m,1}$*	$a_{m,2}$*	$a_{c,1}$*	$a_{c,2}$*	
8	8	4	4	

The consumer outlet temperature responses for the comparison control are illustrated in the top plot of Fig. 4 while the consumer inlet temperatures are shown in the bottom plot of the same figure. For making comparison between the responses for the two control designs easier, the consumer temperature references are included in Fig. 4, even though they are not used by the comparison control design. The top plot of Fig. 5 shows the flow rates for the comparison control during the simulation, while the bottom plot illustrates the corresponding main engine load percentage.

It is clear from the temperature responses for the comparison control in Fig. 4 that the lack of feedback control means the temperatures cannot be controlled to some predefined set points, unless the set points and main engine load percentage are exactly what the comparison control was designed for. The consequence is that the individual consumers does not necessarily operate at optimal conditions as was pointed out in Section I.

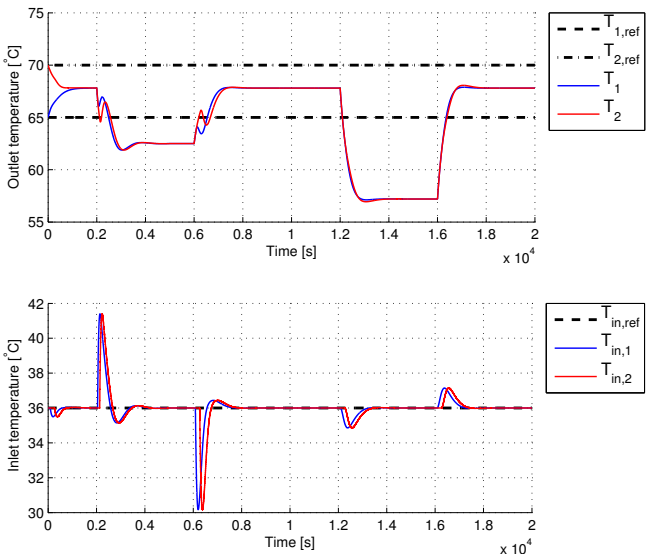

Fig. 4. Top plot illustrates the temperature of the coolant out of the two consumers during the simulation using the comparison control. Bottom plot shows the corresponding consumer inlet temperatures which are identical but displaced in time due to transport delays.

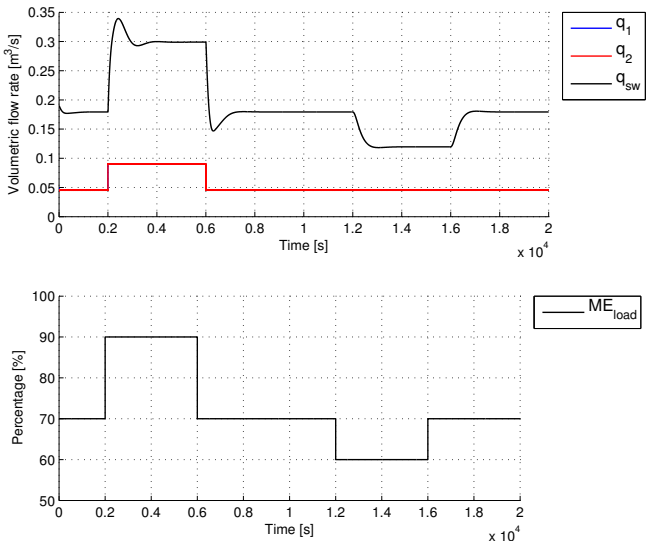

Fig. 5. Top plot illustrates the flow rate through the two consumers and the corresponding SW circuit flow during the simulation using the comparison control. Bottom plot shows the main engine load percentage during the simulation.

Temperature responses for the control designed in this paper are illustrated in Fig. 6, while Fig. 7 shows the corresponding flow rates and main engine load percentage.

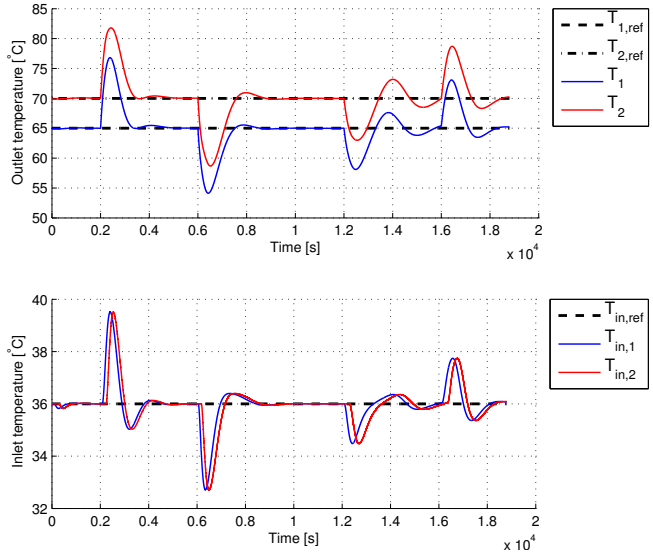

Fig. 6. Top plot illustrates the temperature of the coolant out of the two consumers during the simulation with the control design presented in this paper. Bottom plot shows the corresponding consumer inlet temperatures which are identical but displaced in time due to transport delays.

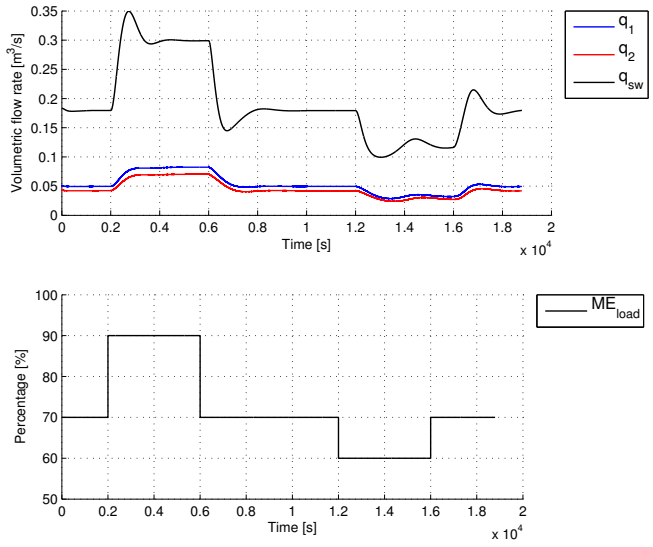

Fig. 7. Top plot illustrates the flow rate through the two consumers and the corresponding SW circuit flow during the simulation using the non-linear model. Bottom plot shows the main engine load percentage during the simulation.

From the temperature responses in Fig. 6 it is seen that the control design presented in this paper is able to bring the consumer outlet temperatures to the defined set points, even when the main engine load percentage does not correspond to the operating point used in the control design. Fig. 6 also illustrates how the nonlinearities causes the compensated system to have a longer settling time during a negative step in the main engine load percentage, compared to a positive step. Compensation for this uneven performance of the control design could possibly be achieved through a nonlinear control design, which however, is outside the scope of this paper.

V. CONCLUSIONS AND FUTURE WORKS

We have presented a simple control design for a non-linear marine cooling system. Control laws were derived using model based control design from the model presented in [5]. The non-linear models were linearized and classical control theory was applied to obtain a cascaded PI controller design.

Through a simulation example the controllers designed in this paper were compared to a control design that is similar in operation to what is currently implemented on the cooling system. The simulation example indicated that the design presented in this paper achieves its purpose of controlling the temperatures in the cooling system to predefined set points, even when disturbances deviates from the chosen operating point. This is an improvement over the comparison control since this is unable to control the system according to set points and reject constant disturbances. Possible improvements for the control design presented here includes ensuring consistent performance in the entire range of operation, i.e. for all possible main engine load percentages and sea water temperatures.

In future work we will look at compensation of the non-linearities, closed circuit flow dynamics and transport delays. Optimization of pump power consumption is another subject that will also be dealt with in future work. The control design derived in this paper will then serve as a performance benchmark for investigating dynamic performance and power consumption.

REFERENCES

[1] C. Beverelli, H. Benamara, and R. Asariotis, "Oil Prices and Maritime Freight Rates: An Empirical Investigation," *United Nations Conference on Trade and Development*, 2010.

[2] J. Faber, A. Markowska, D. Nelissen, M. Davidson, I. C. Eyring, Veronika, P. Roche, E. Humpries, N. Rose, J. Graichen, and M. Cames, "Technical support for european action to reducing greenhouse gas emissions from international maritime transport," *Commissioned by: European Commission*, 2009.

[3] Green Ship of the Future, "Green ship magazine," *www.greenship.org*, 2009.

[4] T. L. Andersen, D. F. Lauritzen, and J. T. Madsen, "Optimized control for energy optimization of shipboard cooling system," *Master thesis, Aalborg University, Section for Automation and Control*, 2009.

[5] M. Hansen, J. Stoustrup, and J. D. Bendtsen, "Modeling of nonlinear marine cooling system with closed circuit flow," *Proceedings of the 18th IFAC World Congress*, 2011.

[6] C. De Persis and C. S. Kallesøe, "Pressure regulation in nonlinear hydraulic networks by positive controls," *European Control Conference*, 2009.

[7] ——, "Proportional and proportional-integral controllers for a nonlinear hydraulic network," *Proceedings of the 17th IFAC World Congress*, 2008.

[8] G. F. Franklin, J. D. Powell, and A. Emami-Naeini, *Feedback Control of Dynamical Systems*. Prentice Hall, 2006.